


## Article

# A Study on the Effect Mechanism of Pectin Modification on the Carrot Cell Wall's Texture Formation under Ultrasonic and Infrared Drying

Kun Gao<sup>1</sup>, Bin Liu<sup>2</sup>, Bengang Wu<sup>1,3,\*</sup> , Yiting Guo<sup>1,3</sup>, Chenyu Song<sup>1</sup>, Shenao Nan<sup>1</sup>, Junjun Dai<sup>1</sup>, Yan Shen<sup>1</sup> and Haile Ma<sup>1,2</sup>

- <sup>1</sup> School of Food and Biological Engineering, Jiangsu University, 301 Xuefu Road, Zhenjiang 212013, China; chinamrgaokun@163.com (K.G.); 1000005604@ujs.edu.cn (Y.G.); songchenyu0222@163.com (C.S.); nan2578399793@163.com (S.N.); daijunjun2023@163.com (J.D.); liand1214@163.com (Y.S.); mhl@ujs.edu.cn (H.M.)
- <sup>2</sup> COFCO Nutrition and Health Research Institute, Beijing 102209, China; liubin11@cofco.com
- <sup>3</sup> Institute of Food Physical Processing, Jiangsu University, 301 Xuefu Road, Zhenjiang 212013, China
- \* Correspondence: wubg@ujs.edu.cn

**Abstract:** The carrot has a high water content, and dehydration is an important means to extend its edible period and reduce storage and transportation costs. In the case of infrared (IR) drying, the porosity of the product is low and the structure is compact; the textural properties of the product are improved by using combined ultrasound and infrared (US-IR) drying; however, there is a lack of reports on the mechanism of this. Pectin has an important influence on the formation of the textural properties of fruit and vegetable tissues. In order to investigate the mechanism of the change in endogenous pectin properties in the carrot cell wall under US-IR drying on the improvement of the textural properties of the product, different fractions of pectins (water-soluble pectin, chelating pectin, alkali-soluble pectin) of the carrot were extracted, separated, and analysed. The thermal stability, component and content changes, Fourier infrared (FTIR), X-ray diffraction (XRD), esterification degree, molecular weight, monosaccharide composition, Ca ion content, and atomic force microscopy (AFM) of the pectins were determined. The results showed that the changes in the contents and properties of the carrot pectins under US-IR conditions had a positive effect on the improvement of the textural properties of the carrot tissues.

**Keywords:** ultrasound; infrared drying; pectin; carrot; texture



**Citation:** Gao, K.; Liu, B.; Wu, B.; Guo, Y.; Song, C.; Nan, S.; Dai, J.; Shen, Y.; Ma, H. A Study on the Effect Mechanism of Pectin Modification on the Carrot Cell Wall's Texture Formation under Ultrasonic and Infrared Drying. *Agriculture* **2024**, *14*, 803. <https://doi.org/10.3390/agriculture14060803>

Academic Editor: Vlasios Goulas

Received: 2 May 2024  
Revised: 15 May 2024  
Accepted: 20 May 2024  
Published: 22 May 2024



**Copyright:** © 2024 by the authors. Licensee MDPI, Basel, Switzerland. This article is an open access article distributed under the terms and conditions of the Creative Commons Attribution (CC BY) license (<https://creativecommons.org/licenses/by/4.0/>).

## 1. Introduction

The carrot is one of the world's leading root vegetables. However, the water content of fresh carrots can be as high as 86% or more, which often results in great resource wastage and economic loss during their storage and transport. Dehydration and drying is currently the most effective method to extend the edible period of carrots and reduce their storage and transport costs [1]. Among the many drying methods, infrared drying (IR) is widely used for fruit and vegetable drying due to its advantages of having high efficiency and good controllability. Wu et al. [2] carried out drying studies on carrot slices using IR and hot air, and found that IR drying has a higher drying rate than hot air drying, and that the products obtained have better rehydration properties. Bi et al. [3] investigated the effect of IR drying on the quality of red dates, and the diffusion coefficient and total flavonoid content of the product were found to be enhanced. However, despite the many advantages of IR drying, the quality of the final product obtained still suffers from some defects due to its wavelength, penetration, and thermal effects. Khampakool et al. [4] studied the IR drying of banana slices and found that the product had a large pore size in the internal region but a dense structure in the surface layer. Our project team has also previously carried

out drying studies on carrot slices using IR, and found that the surface cells of carrots collapsed under IR drying, resulting in irregular deformation and ultimately poor product texture [1]. Obviously, like other individual drying methods, IR drying alone cannot avoid the occurrence of the 'surface hardening phenomenon', and this texture deterioration will seriously affect the diffusion rate of the internal moisture to the outside of the material, so that the internal temperatures of the fruits and vegetables rise too quickly, which will further lead to the loss of nutrients [5,6].

In order to avoid such textural deterioration, our project team conducted drying studies on Jackfruit and carrots using an ultrasound combined with infrared (US-IR) drying method and found that the products obtained were more porous, the cellular structure was retained and more intact, and the textural properties of the products were significantly improved [1,7]. Similar experimental results were also found in US-IR drying studies of potato [8], wolfberry [9], and ginger [10]. In conclusion, the application of an US to the drying of fruits and vegetables has been widely recognised by scholars worldwide, and the effect of USs on the quality enhancement of dried fruits and vegetables as well as on the improvement of the product texture has been intensively studied and reported. However, what is the role of USs in 'regulating' the final textural properties of dried products? The mechanism of improving the textural properties of the products has not been thoroughly investigated, which, to a certain extent, limits the application of USs in the actual drying of fruit and vegetable production.

After reading the literature, we found that among the many factors affecting the textural properties of fruit and vegetable products, changes in cell wall pectin contents and traits are the most important influencing factors. Fruit and vegetable cell walls are mainly composed of pectin, cellulose, hemicellulose, in addition to a small amount of structural proteins, phenolic compounds, etc. [11]. The textural changes during the processing of fruits and vegetables are mainly related to the enzymatic and non-enzymatic degradation of cell wall polysaccharides [12,13], and the changes in the hardness and brittleness of fruits and vegetables are mainly caused by the changes in the structure and components of the cell wall, especially the changes in pectin polysaccharides. In addition, lignin and cellulose are relatively stable in structure during heat treatment, while cell wall pectin is more sensitive to heat processing, and changes in the pectin content and properties during drying can significantly affect the texture of fruits and vegetables [14–16]. Huang et al. [16] showed that the degradation of pectin or the transformation between different types of pectin may be an important factor affecting the texture of fruit and vegetable end-products. De Roeck et al. [17] found that the water-soluble pectin content of carrots increased under a high-temperature treatment, the content of chelating pectin and alkali-soluble pectin decreased, and the texture of the carrots became soft. In conclusion, the changes in the composition and properties of the endogenous pectin in the cell wall during the drying process of fruits and vegetables are importantly related to the formation of the product's texture, and an in-depth study of the effects of USs on the contents and properties of endogenous pectin in the cell wall of carrots is of great significance in revealing the mechanism of US synergistic IR drying in regulating the textures of products.

In this study, carrots were used as the object of study; a contact ultrasonic synergistic infrared simultaneous drying technique was used; a carrot cell wall alcohol-insoluble material (AIR) was extracted and different pectin fractions (water-soluble pectin, chelated pectin, alkali-soluble pectin) were isolated; pectin treated with IR alone was used as a control; the ultrasonic effects on pectin fractions' contents, functional groups, thermal stability, esterification, monosaccharide composition, sugar ratios, and micromorphological properties were analysed, including their molecular weight and microscopic morphology. The  $\text{Ca}^{2+}$  content of the carrot's AIR and surface layer was measured under different drying methods to analyse its effect on the texture of carrot products. From the perspective of pectin modification, the mechanism of the ultrasonic regulation of carrot texture was initially investigated, with an aim to provide a theoretical basis and scientific evidence for the application of ultrasonic waves in fruit and vegetable drying.

## 2. Materials and Methods

### 2.1. Sample Preparation and Equipment

Fresh carrot (variety: Hong Sen) samples were purchased from a local vegetable market in Jingkou District, Zhenjiang, China. Fresh carrots of a uniform size and maturity (about 4 cm in diameter) were selected and placed in a refrigerator at 4 °C. Before the experiment, the carrots were washed and peeled, and the middle part of the carrot samples was selected and sliced into thin slices with a thickness of 5 mm by a food-grade slicer. Figure 1 shows the equipment used in this experiment (the equipment was developed by Jiangsu University, Zhenjiang, China), and the carrot slices were placed in the sample tray (4 slices of carrots at a time, placed in a single layer and not turned over during the drying process) during the experiment. The IR drying distance was 20 cm, the IR power was 1200 W, the contact ultrasonic power was 80 W, the frequency was 20 kHz, and the moisture removal rates of 30%, 40%, and 60% were selected using moisture removal rate as the drying conversion point. The pectin in the samples after individual IR and US-IR drying treatments was extracted and analysed to study the effect of an ultrasound on the pectin components and traits, thus revealing the potential mechanism of an ultrasound's influence on the textural and structural regulation of fruits and vegetables.

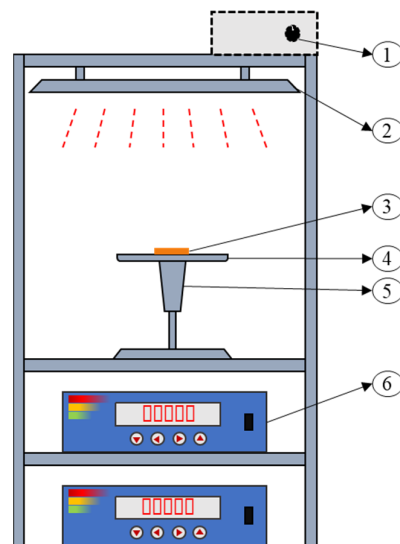


**Figure 1.** A schematic diagram of the ultrasonic synergistic infrared drying equipment. 1. The infrared power regulator; 2. The infrared transmitter; 3. A carrot slice sample; 4. The material tray; 5. The ultrasonic transducer; 6. The ultrasonic generator.

### 2.2. Extraction of Carrot Cell Wall Alcohol-Insoluble Residues

Carrot cell wall alcohol-insoluble residues (AIRs) were extracted referring to the method of Rose et al. [18], with minor modifications. Dried carrot was weighed to be 20 g, 80 mL of a 95% (*v/v*) ethanol solution was added and homogenised for 90 s. The homogenate was transferred to a beaker and stirred magnetically at room temperature for 1 h. The homogenate was filtered via pumping and the beaker was rinsed with 80 mL of a 95% ethanol to extract the filtrate. Add 80 mL of acetone to the filtrate, and put it in a fume hood with magnetic stirring for 1 h. Then, add 80 mL of 95% ethanol and 80 mL of acetone to the filtrate two times, collect the filtrate, and then transfer the filtrate to an oven at 40 °C and bake until it maintains a constant weight, and then obtain the AIR powder.

### 2.3. The Separation and Extraction of Carrot Pectin Fractions

The pectin fractions were separated and extracted by referring to the method of Sila et al. [19], with slight modifications. The dialysis bag (3500 Da, 44 mm) was boiled for 10 min and washed and set aside. Weigh 0.5 g of AIR into 90 mL of distilled water, boil for 10 min, cool to room temperature, and filter. The obtained filtrate was fixed to amount to

100 mL with distilled water, transferred to a dialysis bag, and dialysed in distilled water for 48 h. The water was changed every 12 h. The retained solution was lyophilised to obtain the water-soluble pectin fraction.

The filtrate from the previous step was dissolved in 90 mL of 0.05 mol/L of an EDTA-2Na solution (containing 0.1 mol/L of a sodium acetate solution), filtered after magnetic stirring for 6 h at room temperature, and the resulting filtrate was fixed to amount to 100 mL with distilled water, and transferred to a dialysis bag for dialysis. During the first 24 h, the filtrates were dialysed with 0.1 mol/L of a NaCl solution, and during the second 24 h, the filtrates were dialysed with distilled water, and the dialysate was changed every 12 h. The retention solution was lyophilised to obtain the chelate solution. The retained solution was lyophilised to obtain the chelated pectin fraction.

The filtrate from the previous step was dissolved in 90 mL of 0.05 mol/L of a sodium carbonate ( $\text{Na}_2\text{CO}_3$ ) solution (containing 0.02 mol/L of a sodium borohydride solution), and the filtrate was extracted after magnetic stirring for 2 h at room temperature. The filtrate was volume-determined to amount to 100 mL, and was dialysed in distilled water for 48 h, with water changes every 12 h. The solution was then dried and frozen to obtain the alkaline-soluble solution. The retained solution was lyophilised to obtain the alkali-soluble pectin fraction.

#### 2.4. Fourier-Transform Infrared Spectrometry

The functional group information of the carrot AIR was analysed using attenuated total reflection-Fourier-transform infrared spectroscopy (ATR-FTIR) (Nicolet is50, Thermo Fisher Scientific, Waltham, MA, USA). An appropriate amount of AIR powder was taken at the diamond of the ATR attachment and measured over a scanning range of  $4000\text{--}600\text{ cm}^{-1}$  with a resolution of  $4\text{ cm}^{-1}$  and an average of 32 scans.

#### 2.5. The Thermodynamic Characterisation of Pectin

The thermal stability of the carrot cell wall AIR was determined by a comprehensive thermal analyser (STA 499C, Netzsch Geratebau, Selb, Germany). Prior to the TG/DTG experiments, all samples were dried until they remained a constant weight in an oven at  $40\text{ }^\circ\text{C}$ , about 5 mg of AIR powder was weighed in an uncovered crucible (70  $\mu\text{L}$  SDT-Q/TA6.5), and measured in the temperature range of  $35\text{--}600\text{ }^\circ\text{C}$ , with a ramp rate of  $10\text{ }^\circ\text{C}/\text{min}$ , and a nitrogen flow rate of  $30\text{ mL}/\text{min}$ , to obtain the change in the mass of the samples.

#### 2.6. The X-ray Diffraction of the Carrot Cell Wall-Insoluble Residues

The X-ray diffraction of the carrot AIR powder was determined using a multifunctional high-resolution X-ray diffractometer (SmartLab, Rigaku, Tokyo, Japan). The measurement conditions were as follows: a maximum output power of 9 kW; the target material was a copper target; the detector was a high-resolution, high-speed, two-dimensional, surface-probing direct-reading detector; there was an angular scanning range of  $5\text{--}80^\circ$  ( $2\theta$ ); and a step size of  $0.02^\circ/\text{s}$ ;  $5^\circ/\text{min}$ .

#### 2.7. The Determination of Pectin Esterification

The degree of esterification (DE) of the carrot pectin was determined by referring to the method of Shaha et al. [20], with slight modification; 20 mg of carrot AIR was weighed in a conical flask, moistened with 1 mL of ethanol, and 20 mL of deionised water was added to make it fully soluble. An amount of 200  $\mu\text{L}$  of a 0.5% ( $w/v$ ) phenolphthalein reagent was added dropwise, and the conical flask was shaken in a shaker at  $25\text{ }^\circ\text{C}$  and 150 rpm for 1 h to fully dissolve it. Then, this was titrated with 0.02 mol/L of a NaOH solution until a pink colour appeared for 30 s without fading, and the volume of 0.02 mol/L of a NaOH solution that consumed  $V_1$  was recorded. An amount of 10 mL of a 0.5 mol/L NaOH solution was added, and it was fully saponified by using a shaker under  $25\text{ }^\circ\text{C}$ , at 150 rpm, and shaking vigorously for 2 h. The solution was then dissolved by adding 10 mL of a 0.5 mol/L NaOH

solution, and then shaking it under 25 °C at 150 rpm for 2 h to fully saponify it. An amount of 10 mL of a 0.5 mol/L hydrochloric acid was added to neutralise until the pink colour disappears. Then, it was titrated with 0.02 mol/L of NaOH, and when the pink colour appeared and lasted for 30 s without fading, the titration was ended, and the volume of the 0.02 mol/L NaOH solution that consumed  $V_2$  was recorded. Finally, we calculated the degree of esterification using the following formula:

$$DE = V_2 / (V_1 - V_2) \times 100\% \quad (1)$$

### 2.8. The Determination of the Calcium Ion Content

About 0.5 mm of the upper surface layer of the dried carrot slices was cut for the determination of the calcium ion content of the surface layer of the carrot. The calcium ion content of the surface layer of the carrot was determined via the following method: accurately weighing 1 g of the upper surface layer of the dried carrot slices in the microwave dissolution tank, adding 8 mL of nitric acid and leaving it to stand for 60 min, then covering the safety valve and put the tank into the microwave dissolution instrument. The parameters of microwave digestion were as follows: 20 min of climbing time, 140 °C, 15 min of holding time, half an hour of an acid treatment at 100 °C after digestion, and after the acid treatment, the digestion solution was transferred to a 25 mL volumetric flask. The tank was washed with deionised water, and the washed solution was combined and transferred to a volumetric flask. The standard curve was plotted using the calcium ion standard solution:

$$y = 2.845x + 1.025 \quad (2)$$

where  $R = 0.997$ . The calcium ion content of the samples was determined using inductively coupled plasma mass spectrometry (ICP-MS 2030LF, Shimadzu, Kyoto, Japan). The  $\text{Ca}^{2+}$  content in the carrot cell wall AIR was determined using the following method: 50 mg of AIR powder was weighed accurately, and the digestion and determination methods were the same as those for the determination of the calcium ion content in the surface layer of the carrot slices.

### 2.9. Molecular Weight Determination of Pectin

The weight average of the molecular weight ( $M_w$ ), the number average of the molecular weight ( $M_n$ ), the molecular weight distribution ( $M_w/M_n$ ), and the radius of gyration ( $R_g$ ) of the different fractions of carrot pectins were determined via Size Exclusion Chromatography-Multi-Angle Light Laser Scattering (SEC-MALLS) analysis [21]. An accurately weighed 4 mg pectin sample was dissolved in 4 mL of a 0.1 mol/L NaCl solution (containing 0.02% of a sodium azide ( $\text{NaN}_3$ ) solution), passed through a 0.45  $\mu\text{m}$  aqueous filter membrane, and left to be measured. The detectors included an oscillometric refractive detector (G136A, Agilent Technologies, Inc., Santa Clara, CA, USA) and an octagonal light scattering detector (DAWN HELEOS II, Wyatt, Rocklin, CA, USA); the columns were OHPak SB-806 M HQ and SB-805 HQ in series with OHPak SB-G as a guard column. Data were analysed using Astra version 6.1.7 software.

### 2.10. Analysis of the Pectin's Monosaccharide Composition

The monosaccharide composition of the pectin was determined using high performance liquid chromatography (LC-20AT, Shimadzu, Kyoto, Japan) with a pre-column derivatisation using PMP (1-phenyl-3-methyl-5-pyrazolone). After weighing 2 mg of the pectin into a 10 mL hydrolysis tube, 2 mL of 2 mol/L of trifluoroacetic acid was added for acid hydrolysis, sealed with nitrogen, and hydrolysed in an oven at 110 °C for 6 h. At the end of the hydrolysis, the sample was rotary evaporated to dryness, and then 3 mL of methanol was added to continue the rotary evaporation to dryness, and then added with methanol for evaporation and repeated for four times. The hydrolysed samples were subjected to PMP derivatisation, followed by being passed through a 0.45  $\mu\text{m}$  aqueous membrane and left to be measured.



Standard monosaccharides and standard glucuronides were selected for the preparation of standard curves for qualitative and quantitative analyses. Standard monosaccharides included fucose (Fuc), rhamnose (Rha), arabinose (Ara), galactose (Gal), maltose (Mal), glucose (Glu), xylose (Xyl), mannose (Man); standard glycoalkaloid acids included galacturonic acid (GalA) and glucuronic acid (GluA). The standard curves of various monosaccharides are shown in Table 1.

**Table 1.** The standard curves for the standard monosaccharides and aldoses.

Standard Product	Time of Peak (min)	Standard Curve	R <sup>2</sup>
Mannose	21.053	$y = 2.231 \times 10^{-5}x + 2.370$	0.998
Rhamnose	26.172	$y = 2.954 \times 10^{-5}x + 0.966$	0.998
Glucuronic acid	27.309	$y = 2.834 \times 10^{-5}x + 3.577$	0.997
Galacturonic acid	31.529	$y = 7.101 \times 10^{-5}x + 0.864$	0.996
Glucose	33.458	$y = 3.390 \times 10^{-5}x - 2.968$	0.990
Galactose	36.069	$y = 2.752 \times 10^{-5}x + 1.202$	0.990
Xylose	36.752	$y = 1.909 \times 10^{-5}x + 2.537$	0.990
Arabinose	38.036	$y = 1.728 \times 10^{-5}x + 3.160$	0.990
Fucose	41.237	$y = 3.228 \times 10^{-5}x + 0.223$	0.991

### 2.11. Sugar Ratio Calculation

Sugar ratios were calculated with reference to the method of Houben et al. [22]. In order to interpret the data on the composition of carrot monosaccharides, the polymeric nature of the pectin fraction was characterised by calculating the sugar ratio. The calculation formula is given below:

$$\text{Sugar ratio 1} = \text{GalA} / (\text{Fuc} + \text{Rha} + \text{Ara} + \text{Gal} + \text{Xyl}) \quad (3)$$

$$\text{Sugar ratio 2} = \text{Rha} / \text{GalA} \quad (4)$$

$$\text{Sugar ratio 3} = (\text{Ara} + \text{Gal}) / \text{Rha} \quad (5)$$

Sugar ratio 1 is used to characterise the linearity of the pectin; sugar ratio 2 indicates the percentage of the RG fraction in the pectin polysaccharide; and sugar ratio 3 is used to measure the degree of the branching of the RG-I.

### 2.12. Microscopic Morphology of Pectin

According to the method of Zhang et al. [23], with slight modification, 1 mg of different fractions of carrot pectin was accurately weighed and configured into a 10 µg/mL pectin solution. Twenty µL of the pectin solution (10 µg/mL) was pipetted onto the mica sheet and placed in a fume hood for 2 h. Afterwards, the microscopic morphology of the pectin was scanned using an atomic force microscope (Multimode 8, Bruker, Billerica, MA, USA) in ScanAsyst mode with a scanning range of 1 µm and a scanning frequency of 0.640 Hz. The pectin was then analysed using NanoScope Analysis V1.8 software for offline analysis.

### 2.13. Statistical Analysis

All experiments were repeated at least in triplicate, and data were expressed as the mean ± Standard Deviation (SD). The difference in results was evaluated using a one-way analysis of variance (ANOVA) with Duncan's multiple-range test. All statistical tests were analysed using SPSS 26.0 (IBM Corporation, Chicago, IL, USA) at the significance level of  $p = 0.05$ .

## 3. Results and Discussion

### 3.1. The Effect of Ultrasonic Co-Operative Infrared Drying on the FTIR of Carrot AIR

Infrared spectroscopy is one of the most commonly used spectroscopic techniques for the study of plant cell wall materials, and the combination of Fourier transform and infrared (FT-IR) provides a simple, fast, and sensitive tool for the identification of

compounds [24]. The FT-IR spectra of carrot AIRs under different drying methods are shown in Figure 2. The broad peak at  $3335\text{ cm}^{-1}$  is caused by the hydroxyl ( $-\text{OH}$ ) stretching vibration of polysaccharides or polyphenols, and the absorption peak near  $2900\text{ cm}^{-1}$  is caused by the  $\text{C}-\text{H}$  stretching vibration [25]. The absorption peaks near  $1740\text{ cm}^{-1}$ ,  $1610\text{ cm}^{-1}$ , and  $1235\text{ cm}^{-1}$  are characteristic absorption peaks of pectin, representing the stretching vibrations of the  $\text{C}=\text{O}$  of the free carboxyl group, the  $\text{C}=\text{O}$  of the esterified carboxyl group, and  $\text{C}-\text{O}$ , respectively [26], whereas the absorption peaks near  $1370\text{ cm}^{-1}$  and  $1320\text{ cm}^{-1}$  are caused by the stretching vibrations of  $-\text{CH}_2$  in the dextran linkages and the xylan chains in cellulose and hemicellulose, respectively [24]. The larger absorption peaks occurring near  $1020\text{ cm}^{-1}$  are characteristic absorption peaks of the sugar rings in pectin [26]. Synchronised drying using US-IR did not significantly alter the functional groups in the carrot AIR and its spectral bands were not significantly shifted. In addition, Fourier-transform infrared spectroscopy can be used to analyse the degree of the esterification of the pectin, which can be calculated from the relative area sizes of the absorption peaks located at  $1740\text{ cm}^{-1}$  and  $1610\text{ cm}^{-1}$  [13]. From the peak areas in the figure, it can be seen that the degree of the esterification of the pectin decreased after the application of the US treatment, which is consistent with the results in 3.6 (the effect of the ultrasonic co-operative infrared drying on the change of carrot pectin fraction content). In addition, similar findings were obtained by Hastuti et al. [27].

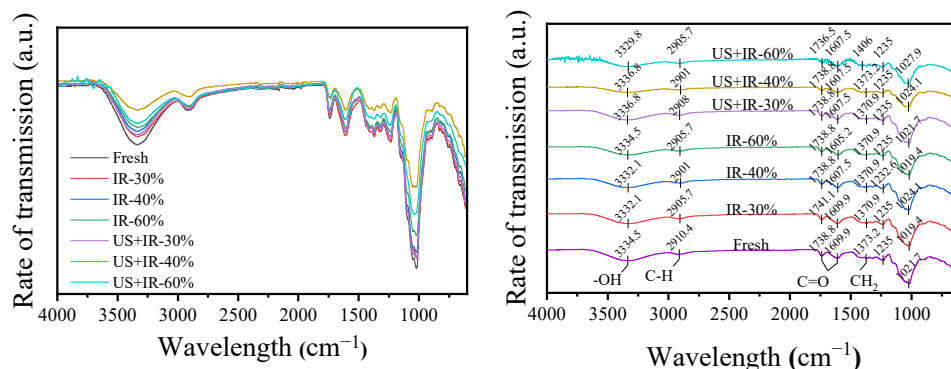


**Figure 2.** The Fourier infrared spectra of the carrot AIRs under different treatment conditions. (Note: ‘Fresh’ denotes fresh samples; IR denotes infrared; US + IR denotes ultrasound combined with infrared; 30%, 40%, and 60% denote the moisture removal amounts, which are the same hereafter).

### 3.2. The Effect of Ultrasonic Co-Operative Infrared Drying on the Thermal Stability of Carrot AIR

Heat treatment causes changes in the basic structure of the cell wall pectin, which affects the textural properties of fruits and vegetables, and it is essential to study the thermal stability of the carrot AIR. Thermogravimetry (TG) is a technique used to analyse the thermal stability of compounds by detecting the change in the sample’s mass with temperature [28]. The AIR-TG curves of the carrot samples for different drying treatments are shown in Figure 3a. The weight loss of the carrot AIRs in the temperature range of  $35\text{--}600\text{ }^{\circ}\text{C}$  for all conditions showed three phases, and similar results have been reported by other researchers [29]. The first stage is within  $35\text{--}180\text{ }^{\circ}\text{C}$ , which corresponds to the loss of water and some volatile compounds, amounting to about 10%; the second stage is within  $180\text{--}400\text{ }^{\circ}\text{C}$ , which is the thermal decomposition of the pectin, the breakage of the glycosidic bond of the galacturonic acid and the decarboxylation of the carboxylic acid moiety, accompanied by the production of various gaseous constituents and gaseous coke, which leads to a rapid loss of mass, amounting to about 55%; and the third stage is within  $400\text{--}600\text{ }^{\circ}\text{C}$ , the stage of slow mass loss, which is mainly brought about by the decomposition of more stable compounds such as cellulose and lignin [30,31]. In the second stage of the TG of the thermal decomposition of pectin, the weight loss of the US synergistically treated AIR was lower, suggesting that carrot pectin is more thermally stable under the action of an ultrasound, which has been attributed by some researchers to structural changes in the pectin [30]. The DTG curves were obtained by taking the first-order derivatives of the TG

curves (e.g., Figure 3b), which is also known as the differential thermogravimetry (DTG) method, and this can more accurately reflect the thermal decomposition behaviours, rates, and thermal stabilities of the samples [32]. The DTG curves of the carrot AIRs from different treatments showed two distinct peaks, which corresponded to the mass loss due to polar small molecules (e.g., water) and pectin degradation, respectively. From the peak shapes and positions of the DTG curves, it can be seen that the samples treated with IR alone reached the temperature of the second stage (pectin degradation) more quickly, indicating that they were less thermally stable. In addition, the rate of pectin degradation was lower for the US co-treated samples at the same temperature.

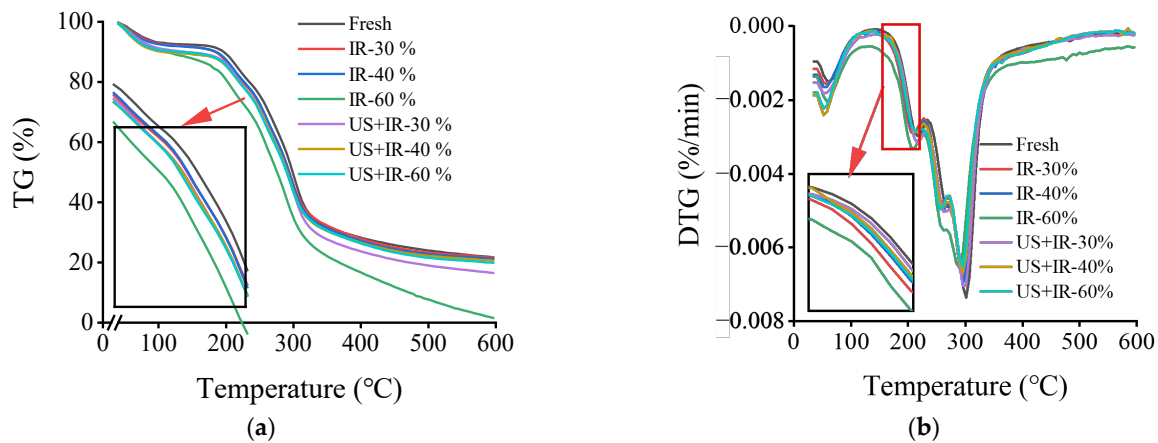


**Figure 3.** The changes in the thermal stability of the carrot AIRs under different treatment conditions. (a) The TG curve; (b) The DTG curve.

### 3.3. The Effect of Ultrasonic Co-Operative Infrared Drying on Carrot AIR X-ray Diffraction

The crystallinity of the carrot AIR powder was determined using X-ray diffraction and the results are shown in Figure 4. All samples were semi-crystalline in nature with a characteristic diffraction peak near  $2\theta$  at  $21.5^\circ$ , indicating that the crystalline structure of the pectin was similar for the different treatments, which is in agreement with the experimental results of Sucheta et al. [25]. Take the example of 60% water removal occurring (Figure 4b) and compare the diffraction peak near  $21.5^\circ$ . The intensities of the peaks of the fresh samples were all increased after the drying treatment, indicating an increase in the crystallinity of the pectin, and it can be observed from the figure that the crystalline peaks of the pectin of the samples treated with IR alone were slightly higher than those of the ultrasonically synergistic condition, but the difference was not significant. Therefore, the effect of an US on the crystallinity of carrot pectin is not significant and the drying treatment has a greater effect on the crystallinity, which corresponds to the results found via FTIR.

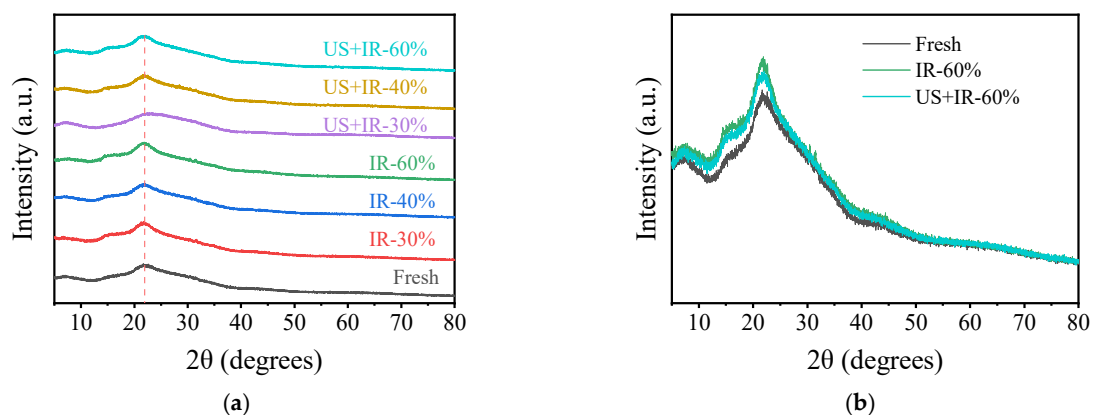


**Figure 4.** X-ray diffraction curves of carrot AIR. (a) X-ray diffraction images of the carrot AIRs under different treatment conditions; (b) X-ray diffraction curves of carrot AIR at 60% water removal.

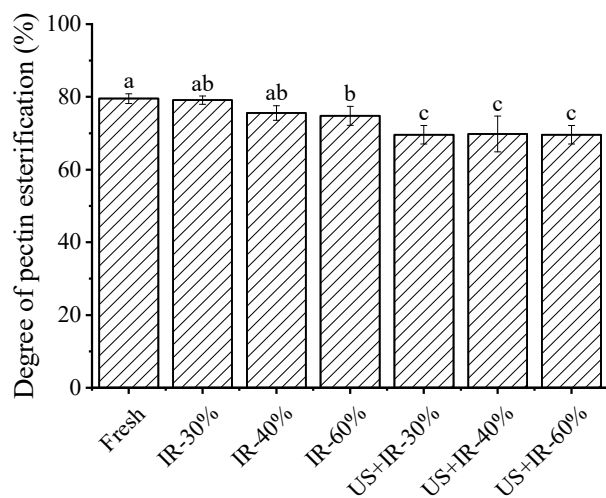


### *3.4. The Effect of Ultrasonic Co-Operative Infrared Drying on the Esterification Degree of Carrot Pectin*

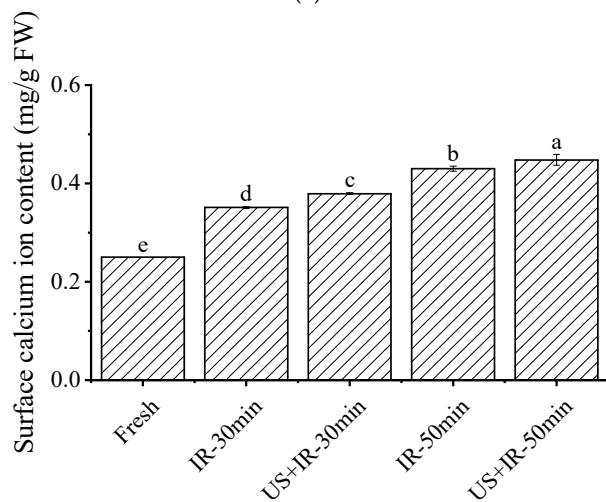
The DE of pectin is of great interest as an important factor in the ability to bind cations and is therefore important to fruit and vegetable textures [33]. The degree of the esterification of the carrot pectin under different treatment conditions is shown in Figure 5a. The esterification degree of fresh carrot pectin was about 79%, which is a high amount of esterification in the pectin. After both the IR and US-IR drying treatments, the degree of the esterification of the carrot pectin decreased. According to Sajjaanantakul et al. [34], this was mainly due to the demethoxylation reaction of pectin at high temperatures. In addition, carrot pectin DE was lower under US-co-operative IR drying, with 12.07%, 7.63%, and 7.00% lower DE at 30%, 40%, and 60% water removal, respectively, compared to the IR drying-alone group, which may be due to the higher temperature during US-IR drying, on the one hand, and the activation of pectin methylesterase inside the carrot by the US, on the other hand. Compared to high methoxy pectin, pectin with low esterification contains more negatively charged carboxyl groups ( $-\text{COOH}$ ), resulting in easier binding with divalent cations such as  $\text{Ca}^{2+}$  to form a cross-linked network structure [35]. Under the action of an US, the binding of pectin with a low esterification to divalent cations can improve the cross-linking of the pectin, which, in turn, improves the inter-cellular adhesion between carrot cells, and therefore the obtained product has a better texture [36,37]. In addition, according to Sila et al. [19] the lower the degree of the esterification of pectin, the worse its water solubility, and completely demethylated pectin showed water insolubility, whereas all carrot pectin esterification degrees decreased after drying treatment, and the decrease in the esterification degree was more significant under US-IR conditions, which implies that the pectin solubility became poorer, which explains the trend of the change in Section 3.6 (the effect of ultrasonic co-operative infrared drying on the change in the carrot pectin fraction content) where a decrease in WSP content occurred.

### *3.5. The Effect of Ultrasonic Co-Operative Infrared Drying on the Calcium Ion Content in the Surface Layer and the AIR of the Carrot Samples*

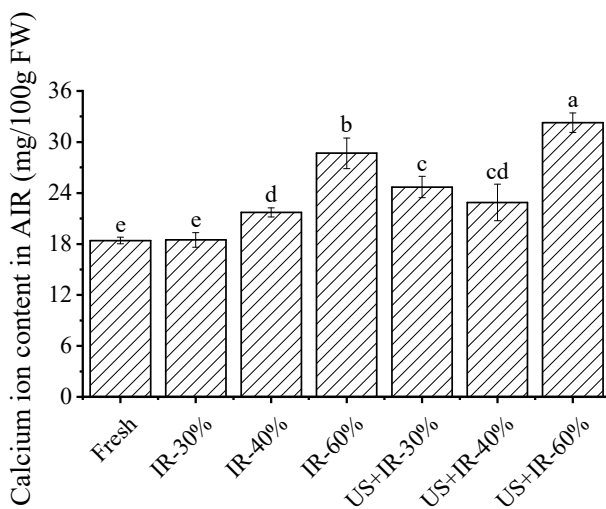
Calcium ions ( $\text{Ca}^{2+}$ ) play an important role in plant cells, where they function as a signal transducer, enabling cells to maintain cell wall integrity in the face of stress [38]. They are also capable of binding to de-esterified pectin to form cross-linked structures, thereby increasing cell wall rigidity [39]. Figure 5b,c shows the  $\text{Ca}^{2+}$  content in the surface layer and the AIR of the carrot slices under different drying conditions. It was found that the  $\text{Ca}^{2+}$  content of the US-IR-drying group was significantly higher than that of the IR-alone group at the same time, and the  $\text{Ca}^{2+}$  content increased by 8% and 4% at drying durations of 30 min and 50 min, respectively, which suggests that CUS promotes  $\text{Ca}^{2+}$ 's migration to the surface of the carrot slices, which may contribute to the improvement of the textural structure of the carrots under US-IR drying conditions. According to Christiaens et al. [37,40],  $\text{Ca}^{2+}$  can be involved in the changes in the textural properties of broccoli by forming cross-linking structures with pectin. In addition, the  $\text{Ca}^{2+}$  content in both the AIR and the surface layers of the carrot slices increased after the application of a drying treatment compared to fresh samples. It was observed that the  $\text{Ca}^{2+}$  content of the carrot AIR under US was higher than that under IR alone at different moisture removal rates, and the  $\text{Ca}^{2+}$  content increased by 33%, 5%, and 12% at the 30%, 40%, and 60% moisture removal rates, respectively. The increase in the  $\text{Ca}^{2+}$  content in the AIR under the effect of an US indicates that more  $\text{Ca}^{2+}$  is retained in the carrot cell wall, making it easier to combine with demethylated pectin, which is involved in the carrot's textural changes [41].



(a)



(b)



(c)

**Figure 5.** Curves of esterification degree and  $\text{Ca}^{2+}$  content of carrot AIR. (a) The carrot pectin esterification under different drying conditions; (b) the calcium ion content in the upper surface layer of the carrot slices; (c) the calcium ion content in the carrot AIR. Note: Letters a–e represent significant differences between the data ( $p < 0.05$ ).

### *3.6. The Effect of Ultrasonic Co-Operative Infrared Drying on the Change in the Carrot Pectin Fraction Content*

Huang et al. [16] showed that the degradation of pectin or the transformation between different types of pectin may be an important factor affecting the texture of fruit and vegetable end-products. The variation in pectin yield is closely related to the drying method, and the yield and the percentage of the components of carrot pectin under different drying methods are shown in Figure 6. The yields of water-soluble pectin (WSP), chelated pectin (CSP), and alkali-soluble pectin (NSP) changed after the drying treatments; the WSP content was found to be higher under IR drying alone, and according to De Roeck et al. [17], the WSP content of carrots increased under high-temperature treatments, while the content of CSP and NSP decreased, and the texture of the carrots became softer, whereas the WSP yield was significantly lower under US-IR conditions, which was attributed to the fact that as drying proceeded, part of the WSP would be leached out with the carrot juice, and part of it would be degraded or transformed with the prolongation of the drying time. It has been shown that the decrease in WSP content during drying leads to a decrease in its supportive effect on the tissue, as well as an increase in the viscoelasticity and plasticity of the tissue, which, together with the faster rate of water dissipation, makes it easier to form more porous structures [42]. In contrast, the increased temperature and water migration rate under US-IR conditions resulted in lower carrot WSP yields and higher CSP and NSP yields compared to those under IR drying. In an intact cell wall structure, WSP is cross-linked to the cell wall through non-covalent or non-ionic bonds, CSP binds to calcium ions in the cell wall through ionic bonds, and NSP binds to cell wall polysaccharides such as cellulose and hemicellulose through covalent bonds [14,43]. Obviously, CSP and NSP are more cross-linked with cell wall substances. It has been shown that CSP plays a key role in the formation and maintenance of the textures of fruit and vegetable products, and its content is positively correlated with hardness, and NSP content is also positively correlated with the hardness of fruits and vegetables, while, on the contrary, WSP content is negatively correlated with hardness [17]. Combined with the changes in the percentage of pectin fractions (Figure 6d), it can be found that the proportion of CSP and NSP increased significantly under US-IR conditions, while the proportion of WSP decreased significantly, which may also be the reason for the better quality of carrot texture under US-IR conditions.

### *3.7. The Effect of Ultrasonic Co-Operative Infrared Drying on the Monosaccharide Composition and the Sugar Ratio of Carrot Pectin*

Pectin is a structurally complex polysaccharide with galacturonic acid (GalA) as its main chain, different types of monosaccharides attached to its main chain in various ways to form side chains, and researchers have cumulatively isolated and identified 17 monosaccharides from pectin [42,44]. Since some of the monosaccharides are very low in pectin, we therefore selected seven types of monosaccharides and two types of uronic acids to be analysed in this study. The results of the changes in the neutral sugar and uronic acid contents of the carrot pectin under different drying methods are shown in Table 2. The neutral sugar and uronic acid contents of the carrot pectin varied significantly with different drying methods. GalA, for example, is the main constituent unit of pectin, so it can be used to measure the content change of a certain pectin. Under IR drying alone, the GalA content of WSP was higher, indicating that pectin mostly existed in the form of hypergalacturonic acid glycan (HG), and the pectin content and linearity of WSP were higher. In contrast, the GalA content of WSP was significantly lower under ultrasonication conditions compared to IR alone, while the GalA content of CSP was significantly higher, indicating that WSP was severely degraded and partially transformed into CSP with a higher chelating capacity, which is consistent with the results of the change in pectin fractions in Section 3.6.

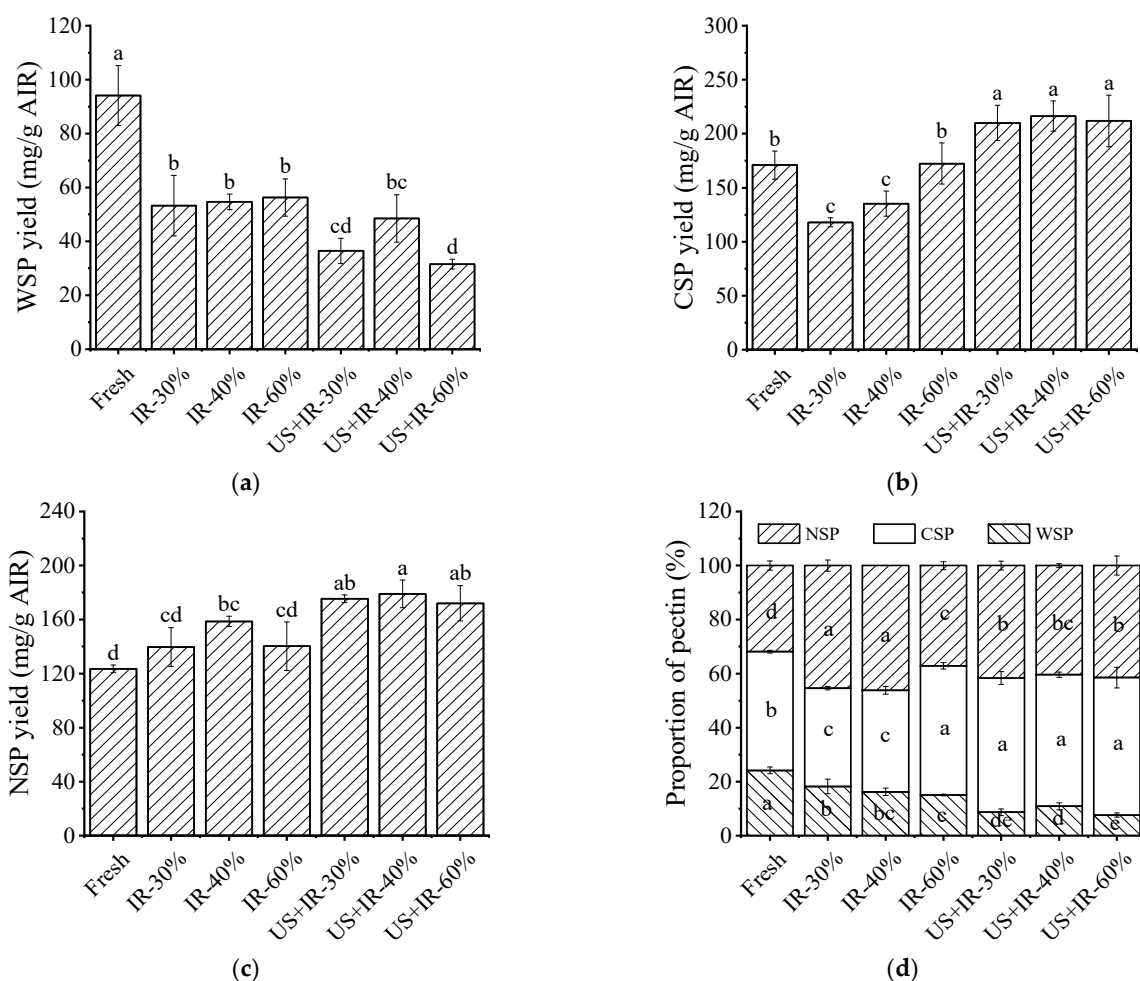


**Figure 6.** Carrot pectin yield and percentage under different drying conditions. (a) WSP yield; (b) CSP yield; (c) NSP yield; and (d) fraction proportions of different pectins. Note: Letters a–e represent significant differences between the data ( $p < 0.05$ ).

**Table 2.** The contents of the neutral sugars and uronic acids of the three fractions of pectin extracted from the carrots under various blanching conditions.

Pectin Types	Conditions	The Contents of Neutral Sugars and Uronic Acids (mg/g AIR)								
		Man	Rha	Glu	Man	Xyl	Ara	Man	GluA	GalA
WSP	Fresh	2.36 ± 0.2 e	3.42 ± 0.4 h	2.81 ± 1.0 bc	14.07 ± 3.1 l	8.66 ± 1.0 k	6.40 ± 0.1 b	0.78 ± 0.1 fg	2.10 ± 0.2 i	38.79 ± 2.7 klm
	IR-30%	2.63 ± 0.0 d	3.26 ± 1.2 h	264.74 ± 34.0 a	20.03 ± 0.3 k	8.24 ± 0.2 k	5.45 ± 0.1 c	5.03 ± 0.1 a	2.39 ± 0.0 h	47.22 ± 1.2 hi
	IR-40%	2.60 ± 0.1 d	3.45 ± 0.2 h	5.45 ± 0.1 bc	23.61 ± 0.9 ij	9.92 ± 0.1 j	4.32 ± 0.2 d	0.57 ± 0.2 gh	2.01 ± 0.1 i	36.67 ± 0.8 lm
	IR-60%	5.30 ± 0.1 a	5.25 ± 0.0 g	265.38 ± 0.8 a	26.46 ± 0.3 gh	10.72 ± 0.4 j	0.71 ± 0.0 n	0.54 ± 0.3 gh	2.83 ± 0.0 g	48.24 ± 1.0 h
	US + IR-30%	3.05 ± 0.1 b	1.48 ± 0.1 i	2.54 ± 0.4 c	15.47 ± 0.8 i	5.58 ± 0.4 l	3.37 ± 0.1 f	0.10 ± 0.0 ij	1.08 ± 0.1 k	21.11 ± 1.1 n
	US + IR-40%	3.13 ± 0.0 b	0.96 ± 0.0 ij	3.19 ± 0.1 bc	11.91 ± 0.1 m	5.51 ± 0.0 l	2.28 ± 0.0 i	0.05 ± 0.0 j	1.12 ± 0.0 k	18.70 ± 0.0 n
	US + IR-60%	2.76 ± 0.0 c	0.59 ± 0.0 j	2.78 ± 0.0 bc	8.46 ± 0.0 n	3.74 ± 0.0 m	0.87 ± 0.0 m	0.06 ± 0.0 ij	0.79 ± 0.0 l	5.14 ± 0.0 o
CSP	Fresh	1.94 ± 0.1 g	9.02 ± 0.2 d	1.56 ± 0.1 c	27.79 ± 0.0 g	17.17 ± 0.0 g	2.16 ± 0.0 i	1.09 ± 0.1 def	3.07 ± 0.1 f	108.19 ± 2.7 b
	IR-30%	1.41 ± 0.0 k	2.69 ± 0.4 h	2.85 ± 0.4 bc	6.78 ± 1.3 n	7.95 ± 0.8 k	7.38 ± 0.2 a	0.46 ± 0.2 ghi	1.73 ± 0.0 j	40.23 ± 2.8 jkl
	IR-40%	1.61 ± 0.0 ij	5.21 ± 0.2 g	0.90 ± 0.0 c	19.31 ± 0.2 k	15.56 ± 0.2 h	1.71 ± 0.0 kl	0.61 ± 0.3 g	2.42 ± 0.1 h	82.85 ± 3.5 d
	IR-60%	2.39 ± 0.0 e	5.45 ± 0.1 fg	ND	14.32 ± 1.7 l	13.00 ± 0.9 i	3.04 ± 0.0 g	1.12 ± 0.1 defg	3.50 ± 0.0 c	74.85 ± 9.4 e
	US + IR-30%	2.82 ± 0.0 c	6.18 ± 0.0 ef	ND	22.79 ± 0.1 ij	16.86 ± 0.4 g	2.86 ± 0.0 h	1.48 ± 0.4 cd	3.97 ± 0.0 a	114.24 ± 3.4 b
	US + IR-40%	2.64 ± 0.0 d	6.11 ± 0.1 ef	ND	22.31 ± 0.1 j	19.22 ± 0.2 f	2.73 ± 0.0 h	1.33 ± 0.14 cde	3.68 ± 0.0 b	90.90 ± 0.9 c
	US + IR-60%	2.39 ± 0.0 e	4.87 ± 0.0 g	ND	18.93 ± 0.3 k	15.10 ± 0.3 h	2.18 ± 0.0 i	0.79 ± 0.2 f	3.22 ± 0.0 e	138.21 ± 0.6 a
NSP	Fresh	1.52 ± 0.0 j	18.53 ± 0.2 a	16.51 ± 0.0 b	92.49 ± 0.2 b	37.93 ± 0.0 c	1.58 ± 0.0 l	1.39 ± 0.6 cde	2.81 ± 0.1 g	47.60 ± 2.1 hi
	IR-30%	1.66 ± 0.0 hi	18.79 ± 0.3 a	ND	107.70 ± 0.1 a	60.62 ± 0.2 a	1.77 ± 0.0 k	2.00 ± 0.1 b	2.93 ± 0.1 g	45.34 ± 2.1 hij
	IR-40%	1.75 ± 0.0 h	15.64 ± 0.2 b	ND	79.14 ± 0.1 c	42.63 ± 0.2 b	2.01 ± 0.0 j	1.55 ± 0.1 c	3.31 ± 0.1 e	54.16 ± 3.6 g
	IR-60%	1.74 ± 0.0 h	12.55 ± 0.4 c	ND	66.43 ± 0.3 d	38.69 ± 0.2 c	1.77 ± 0.0 k	1.44 ± 0.0 cde	2.87 ± 0.1 g	43.19 ± 2.9 ijk
	US + IR-30%	1.95 ± 0.1 g	6.78 ± 1.3 e	0.04 ± 0.0 c	24.82 ± 3.5 hi	17.38 ± 1.2 g	3.70 ± 0.1 e	0.19 ± 0.0 hij	2.83 ± 0.0 g	36.19 ± 0.7 m
	US + IR-40%	2.10 ± 0.0 f	12.34 ± 0.1 c	ND	58.39 ± 0.1 e	34.44 ± 0.0 d	2.26 ± 0.0 i	1.07 ± 0.0 ef	3.46 ± 0.0 cd	59.62 ± 0.0 f
	US + IR-60%	2.15 ± 0.0 f	9.72 ± 0.0 d	ND	37.33 ± 0.2 f	26.94 ± 0.0 e	2.17 ± 0.0 i	1.29 ± 0.1 cde	3.34 ± 0.0 de	55.79 ± 0.2 fg

Note: ND: Not detected. Different letters in the same column indicate significant differences between the data ( $p < 0.05$ ).

In order to better interpret the results of the monosaccharide composition, the sugar ratios were calculated as shown in Table 3, which can reflect the structural information

of pectin. Sugar ratio 1 can reflect the linearity of the pectin; sugar ratio 2 can reflect the change in the main chain, i.e., the proportion of the Rhamnogalacturonan (RG)-type of pectin in the whole pectin; and sugar ratio 3 reflects the ratio of the RG-I-branched chain to the Rha [45]. As can be seen from the table, the linearity of the WSP molecules decreased under all conditions, while the linearity of CSP and NSP increased to varying degrees, suggesting that the chain of WPS molecules was broken during drying, which resulted in its conversion to CSP. In addition, WSP had the highest degree of branching among the different pectins; this made it less bound to other substances in the cell wall and easier to extract. Compared to IR drying alone, WSP molecules were less linear and more branched under US-IR drying; the percentage of RG-I pectin decreased in the CSP; and NSP was more linear, had less RG-I pectin, and was less branched. Combined with the change in the esterification degree, it was speculated that the carrots under ultrasonication had better textural properties probably due to the fact that the longer pectin molecular chain and the lower number of branched chains under the low esterification degree made it easier to cross-link with  $\text{Ca}^{2+}$  [46].

**Table 3.** The sugar ratios of the three fractions of pectin extracted from the carrots under various blanching conditions.

Pectin Types	Conditions	Ratio of Sugars		
		1	2	3
WSP	Fresh	1.164	0.088	5.981
	IR-30%	1.124	0.069	7.804
	IR-40%	0.876	0.094	8.088
	IR-60%	1.104	0.109	5.178
	US + IR-30%	0.812	0.070	12.762
	US + IR-40%	0.902	0.051	14.786
	US + IR-60%	0.375	0.114	15.851
CSP	Fresh	1.890	0.083	3.320
	IR-30%	1.593	0.067	5.269
	IR-40%	1.954	0.063	4.039
	IR-60%	2.491	0.059	3.185
	US + IR-30%	2.277	0.054	4.152
	US + IR-40%	1.758	0.067	4.101
	US + IR-60%	2.685	0.043	4.331
NSP	Fresh	0.313	0.389	5.076
	IR-30%	0.238	0.414	5.824
	IR-40%	0.384	0.289	5.189
	IR-60%	0.357	0.291	5.433
	US + IR-30%	0.685	0.187	4.209
	US + IR-40%	0.549	0.207	4.914
	US + IR-60%	0.720	0.174	4.065

### 3.8. The Effect of Ultrasonic Co-Operative Infrared Drying on the Molecular Weight of Carrot Pectin

The molecular weight of pectin is closely related to its rheological properties, gel properties, bioactivity, and ion-binding capacity [35]. The changes in the molecular weight of carrot pectin under different drying conditions are detailed in Table 4. The molecular weights (Mws) of the WSP and NSP of the fresh samples were lower, while the Mw of CSP was the largest, and the Mws/Mns of WSP, CSP, and NSP were 1.575 ( $\pm 1.722\%$ ), 1.735 ( $\pm 1.369\%$ ), and 2.227 ( $\pm 2.386\%$ ), respectively, which indicated that the molecular weight distributions were more concentrated, and the polymers were of a high purity and more consistent with the length of the pectin chains. The decrease in the Mw of WSP under IR conditions may be due to the occurrence of the  $\beta$ -elimination reaction, where the molecular chain is broken, resulting in a smaller molecular weight. The Mw of WSP became larger under US conditions, which may be related to the conversion of WSP to CSP or NSP. The CSP's Mw became larger after drying, and the molecular weight of CSP



under the US condition was larger than that under the IR alone, and the distribution was more concentrated, while, according to Sila et al. [14], the larger the molecular weight of the pectin, the more significant its cross-linking effect. Combined with the changes in the contents of the pectin components, the WSP content accounted for a small percentage under US-IR conditions, but the molecular weight was larger; the NSP's molecular weight was small but its content accounted for a large percentage. And, according to the Mw/Mn, the molecular weight distribution of CSP and NSP was more uniform and concentrated and the polymer state was purer under US-IR conditions compared to the IR alone, and a similar situation occurred in the US treatment of apple pectin [47]. From the root mean square radius of the rotation (Rg) of the three fractions of pectin, the Rg values of WSP and NSP were comparable in the two drying conditions, whereas the Rg of CSP was the largest in the US condition, which may be related to the length of the molecular chain of the pectin polymers, and this is also related to the degree of branching of the pectin.

**Table 4.** The molecular weights of the carrot pectin fractions under different drying conditions.

Pectin Types		Mw ( $\times 10^5$ Da)	Mn ( $\times 10^5$ Da)	Mw/Mn	Rg(nm)
WSP	Fresh	1.815 ( $\pm 0.72\%$ )	1.152 ( $\pm 1.56\%$ )	1.575 ( $\pm 1.72\%$ )	42.5 ( $\pm 3.7\%$ )
	IR-60%	1.709 ( $\pm 1.08\%$ )	1.045 ( $\pm 1.00\%$ )	1.636 ( $\pm 1.47\%$ )	52.1 ( $\pm 3.7\%$ )
	US + IR-60%	3.550 ( $\pm 0.64\%$ )	1.707 ( $\pm 0.77\%$ )	2.080 ( $\pm 1.00\%$ )	50.9 ( $\pm 2.3\%$ )
CSP	Fresh	3.029 ( $\pm 0.71\%$ )	1.746 ( $\pm 1.17\%$ )	1.735 ( $\pm 1.37\%$ )	64.8 ( $\pm 1.7\%$ )
	IR-60%	3.303 ( $\pm 0.73\%$ )	2.068 ( $\pm 1.18\%$ )	1.597 ( $\pm 1.39\%$ )	73.1 ( $\pm 1.4\%$ )
	US + IR-60%	3.495 ( $\pm 1.10\%$ )	2.643 ( $\pm 1.22\%$ )	1.322 ( $\pm 1.65\%$ )	85.8 ( $\pm 1.6\%$ )
NSP	Fresh	1.216 ( $\pm 0.90\%$ )	5.463 ( $\pm 2.21\%$ )	2.227 ( $\pm 2.39\%$ )	45.4 ( $\pm 4.0\%$ )
	IR-60%	5.679 ( $\pm 0.42\%$ )	1.962 ( $\pm 1.23\%$ )	2.895 ( $\pm 1.30\%$ )	55.4 ( $\pm 1.3\%$ )
	US + IR-60%	2.858 ( $\pm 0.90\%$ )	1.212 ( $\pm 2.39\%$ )	2.358 ( $\pm 2.55\%$ )	55.8 ( $\pm 2.7\%$ )

### 3.9. The Effect of Ultrasonic Co-Operative Infrared Drying on the Micro-Morphological Changes in Carrot Pectin

Atomic force microscopy (AFM) is capable of observing microstructures from a micrometre to a nanometre scale, and it reflects the undulation of the sample surface through the change in the interaction force between atoms, which is very suitable for the observation of the microscopic morphology of pectin in this study [48]. The atomic force microscopy images of the different components of pectin are shown in Figure 7. Fresh carrot WSP was aggregated and showed relatively obvious nodes, which is consistent with the results reported by Cybulska et al. [49] for carrot WSP, and is usually caused by intermolecular interactions [50]. The appearance of some chain-like structures in WSP after IR drying alone suggests the possibility of depolymerisation. In contrast, the WSP under US conditions showed the worst degree of cross-linking, breaking into very small structures. For the CSP fraction, fresh CSP showed a reticulated structure with thick pectin chains and some cross-linking. Some aggregates appeared after IR drying alone, but the pectin chains became finer and partially broken, suggesting that some degree of degradation may have occurred as well. In contrast, the CSP under the US-IR drying better maintained the original morphological characteristics. The NSP of the fresh samples had obvious main chains and side chains, and the degree of aggregation was large, forming very thick and obvious aggregated chains, and the chain height value was the largest. As drying proceeded, the NSP chains began to depolymerise from the aggregates and the entanglement of the side chains could be observed. The NSP chains under different conditions showed a regular mesh structure cross-linked with each other, but the NSP was more dense under the US conditions, and Cybulska et al. [49] showed that this NSP structure may be typical for fruits and vegetables.

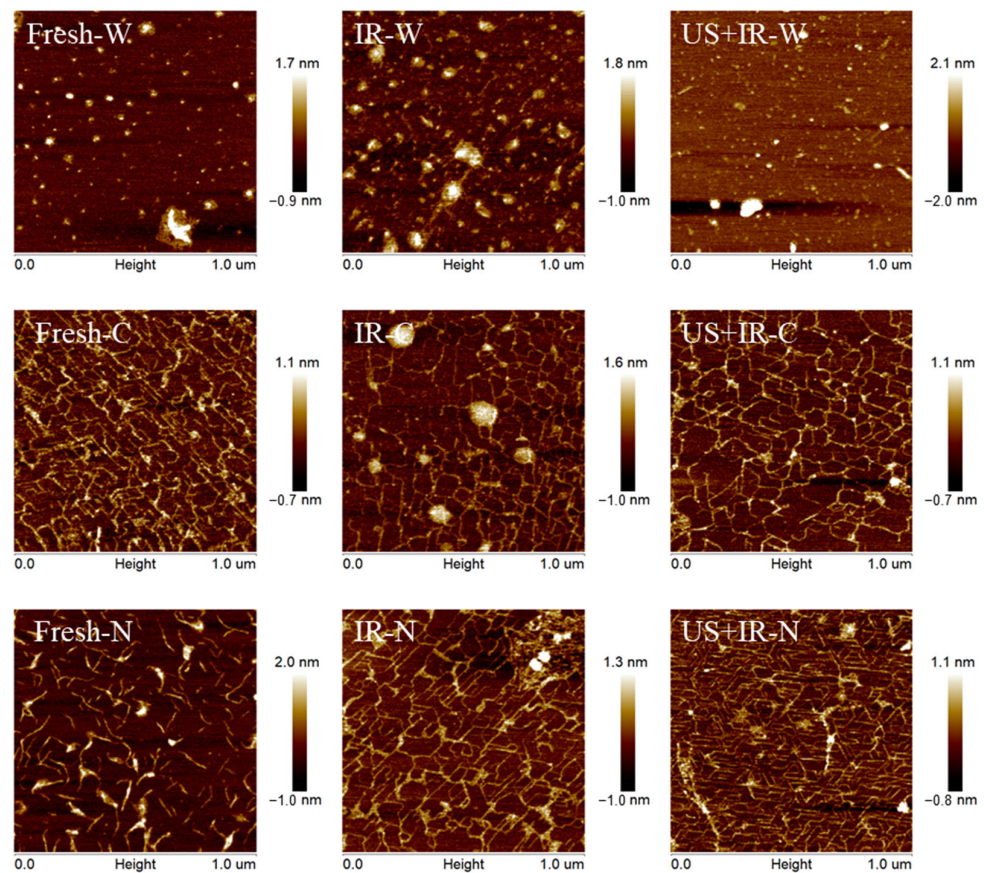


**Figure 7.** AFM images of carrot pectins under various drying conditions. (Note: IR is infrared drying alone; US + IR is ultrasonic cooperative infrared drying; W denotes WSP, C denotes CSP, N denotes NSP).

#### 4. Conclusions

In this study, the mechanism of action for the improvement of the texture and structure of the carrot slices under US-IR drying was investigated from the point of view of the changes in the traits of endogenous pectins in the cell wall, using carrots as the object of study. The component content, functional groups, thermal stability, esterification, monosaccharide composition, sugar ratio, molecular weight, and microscopic morphology of carrot AIR as well as the WSP, CSP, and NSP amounts and features were analysed using IR-treated pectin alone as a control. The  $\text{Ca}^{2+}$  content of the carrot AIR and surface layer under different drying methods was determined to analyse its effect on the texture of carrot products. It was found that the yield and percentage of WSP in carrot slices was significantly reduced under US conditions, while the yields and percentages of CSP and NSP were increased, resulting in higher intercellular adhesion and the carrot slices being less susceptible to intercellular sliding deformation. The monosaccharide composition showed a significant decrease in the galacturonic acid content of WSP and a significant increase in the galacturonic acid content of CSP, suggesting that the US facilitated the conversion between pectin fractions. The DE of the pectin was significantly reduced under US-IR drying, and the sugar ratio analysis revealed that the CSP and NSP had high degrees of linearity and low degrees of branching, which was conducive to the cross-linking of pectin with divalent cations. In addition, the  $\text{Ca}^{2+}$  content in the AIR was significantly higher under US-IR drying, as well as the  $\text{Ca}^{2+}$  content in the surface layer of the carrot slices, suggesting that  $\text{Ca}^{2+}$  may be retained in the carrot cell wall in a bound form, thus improving the textural properties of the carrots. However, X-ray diffraction and FTIR results did not reveal the generation of new functional group structures. In conclusion, US-IR drying had a large effect on the components, contents, and properties of the carrot pectin, and the changes in these factors played a positive role in the adhesion between cells and the stability of the

cellular structure, which may be an important factor in the improvement of the textural properties of fruits and vegetables (the porosity of the product, its microstructure, and its rehydration, etc.) by using USs in drying. The preliminary elucidation of this mechanism is important for the further development of the use of USs in fruit and vegetable drying.

**Author Contributions:** Conceptualization, K.G.; Methodology, K.G., B.L., B.W. and Y.G.; validation, K.G. and B.L.; formal analysis, K.G.; data curation, K.G.; Writing—Review and Editing, K.G., B.L., B.W., C.S., S.N., J.D., Y.S. and H.M.; visualization, K.G.; funding acquisition, B.W. and Y.G.; supervision, B.W. and Y.G.; project administration, B.W. and Y.G. All authors have read and agreed to the published version of the manuscript.

**Funding:** This work was supported by funding from the National Natural Science Foundation of China (No. 32202091) and the China Postdoctoral Science Foundation (No. 2021M700908; No. 2022TQ0128; No. 2022M721388).

**Institutional Review Board Statement:** Not applicable.

**Data Availability Statement:** The original contributions presented in the study are included in the article material, further inquiries can be directed to the corresponding author.

**Conflicts of Interest:** The authors (including Bin Liu) declare that they have no known competing financial interests or personal relationships that could have appeared to influence the work reported in this paper. The author “Bin Liu” and the affiliated company “COFCO Nutrition and Health Research Institute, China” have no financial or other conflicts of interest with the other authors of this article or the content of this article.

## References

- Guo, Y.; Wu, B.; Guo, X.; Ding, F.; Pan, Z.; Ma, H. Effects of Power Ultrasound Enhancement on Infrared Drying of Carrot Slices: Moisture Migration and Quality Characterizations. *LWT-Food Sci. Technol.* **2020**, *126*, 109312. [[CrossRef](#)]
- Wu, B.; Ma, H.; Qu, W.; Wang, B.; Zhang, X.; Wang, P.; Wang, J.; Atungulu, G.; Pan, Z. Catalytic Infrared and Hot Air Dehydration of Carrot Slices. *J. Food Process Eng.* **2014**, *37*, 111–121. [[CrossRef](#)]
- Bi, J.; Chen, Q.; Zhou, Y.; Liu, X.; Wu, X.; Chen, R. Optimization of Short- and Medium-Wave Infrared Drying and Quality Evaluation of Jujube Powder. *Food Bioprocess Technol.* **2014**, *7*, 2375–2387. [[CrossRef](#)]
- Khampakool, A.; Soisungwan, S.; Park, S.H. Potential Application of Infrared Assisted Freeze Drying (Irafd) for Banana Snacks: Drying Kinetics, Energy Consumption, and Texture. *LWT-Food Sci. Technol.* **2019**, *99*, 355–363. [[CrossRef](#)]
- Khan MI, H.; Karim, M.A. Cellular Water Distribution, Transport, and Its Investigation Methods for Plant-Based Food Material. *Food Res. Int.* **2017**, *99*, 1–14. [[CrossRef](#)] [[PubMed](#)]
- Prothon, F.; Ahrné, L.M.; Sjöholm, I. Mechanisms and Prevention of Plant Tissue Collapse During Dehydration: A Critical Review. *Crit. Rev. Food Sci. Nutr.* **2003**, *43*, 447–479. [[CrossRef](#)]
- Wu, B.; Guo, X.; Guo, Y.; Ma, H.; Zhou, C. Enhancing Jackfruit Infrared Drying by Combining Ultrasound Treatments: Effect on Drying Characteristics, Quality Properties and Microstructure. *Food Chem.* **2021**, *358*, 129845. [[CrossRef](#)] [[PubMed](#)]
- Xi, H.; Liu, Y.; Guo, L.; Hu, R. Effect of Ultrasonic Power on Drying Process and Quality Properties of Far-Infrared Radiation Drying on Potato Slices. *Food Sci. Biotechnol.* **2020**, *29*, 93–101. [[CrossRef](#)] [[PubMed](#)]
- Zhang, Q.; Wan, F.; Zang, Z.; Jiang, C.; Xu, Y.; Huang, X. Effect of Ultrasonic Far-Infrared Synergistic Drying on the Characteristics and Qualities of Wolfberry (*Lycium barbarum* L.). *Ultrason. Sonochem.* **2022**, *89*, 106134. [[CrossRef](#)]
- Feng, Z.; Zhang, M.; Guo, L.; Shao, R.; Wang, X.; Liu, F. Effect of Direct-Contact Ultrasonic and Far Infrared Combined Drying on the Drying Characteristics and Quality of Ginger. *Processes* **2024**, *12*, 98. [[CrossRef](#)]
- Keegstra, K. Plant Cell Walls. *Plant Physiol.* **2010**, *154*, 483–486. [[CrossRef](#)] [[PubMed](#)]
- Sila, D.N.; Duvetter, T.; De Roeck, A.; Verlent, I.; Smout, C.; Moates, G.K.; Hills, B.P.; Waldron, K.K.; Hendrickx, M.; Van Loey, A. Texture Changes of Processed Fruits and Vegetables: Potential Use of High-Pressure Processing. *Trends Food Sci. Technol.* **2008**, *19*, 309–319. [[CrossRef](#)]
- Kyomugasho, C.; Christiaens, S.; Shpigelman, A.; Van Loey, A.M.; Hendrickx, M.E. Ft-Ir Spectroscopy, a Reliable Method for Routine Analysis of the Degree of Methylesterification of Pectin in Different Fruit- and Vegetable-Based Matrices. *Food Chem.* **2015**, *176*, 82–90. [[CrossRef](#)] [[PubMed](#)]
- Sila, D.N.; Doungla, E.; Smout, C.; Van Loey, A.; Hendrickx, M. Pectin Fraction Interconversions: Insight into Understanding Texture Evolution of Thermally Processed Carrots. *J. Agric. Food Chem.* **2006**, *54*, 8471–8479. [[CrossRef](#)]
- Liu, J.; Bi, J.; McClements, D.J.; Liu, X.; Yi, J.; Lyu, J.; Zhou, M.; Verkerk, R.; Dekker, M.; Wu, X.; et al. Impacts of Thermal and Non-Thermal Processing on Structure and Functionality of Pectin in Fruit- and Vegetable- Based Products: A Review. *Carbohydr. Polym.* **2020**, *250*, 116890. [[CrossRef](#)]



16. Huang, L.-L.; Zhang, M.; Wang, L.-P.; Mujumdar, A.S.; Sun, D.-F. Influence of Combination Drying Methods on Composition, Texture, Aroma and Microstructure of Apple Slices. *LWT-Food Sci. Technol.* **2012**, *47*, 183–188. [[CrossRef](#)]
17. De Roeck, A.; Sila, D.N.; Duvetter, T.; Van Loey, A.; Hendrickx, M. Effect of High Pressure/High Temperature Processing on Cell Wall Pectic Substances in Relation to Firmness of Carrot Tissue. *Food Chem.* **2008**, *107*, 1225–1235. [[CrossRef](#)]
18. Rose, J.K.; Hadfield, K.A.; Labavitch, J.M.; Bennett, A.B. Temporal Sequence of Cell Wall Disassembly in Rapidly Ripening Melon Fruit. *Plant Physiol.* **1998**, *117*, 345–361. [[CrossRef](#)]
19. Sila, D.N.; Smout, C.; Elliot, F.; Van Loey, A.; Hendrickx, M. Non-Enzymatic Depolymerization of Carrot Pectin: Toward a Better Understanding of Carrot Texture During Thermal Processing. *J. Food Sci.* **2006**, *71*, E1–E9. [[CrossRef](#)]
20. Shaha, R.K.; Punichelvana, Y.; Afandi, A. Optimized Extraction Condition and Characterization of Pectin from Kaffir Lime (*Citrus Hystrix*). *Res. J. Agric. For. Sci.* **2013**, *2320*, 6063.
21. Chen, T.; Zhang, Z.; Wang, Z.; Chen, Z.-L.; Ma, H.; Yan, J.-K. Effects of Ultrasound Modification at Different Frequency Modes on Physicochemical, Structural, Functional, and Biological Properties of Citrus Pectin. *Food Hydrocoll.* **2021**, *113*, 106484. [[CrossRef](#)]
22. Houben, K.; Jolie, R.P.; Fraeye, I.; Van Loey, A.M.; Hendrickx, M.E. Comparative Study of the Cell Wall Composition of Broccoli, Carrot, and Tomato: Structural Characterization of the Extractable Pectins and Hemicelluloses. *Carbohydr. Res.* **2011**, *346*, 1105–1111. [[CrossRef](#)]
23. Zhang, M.; Qin, H.; An, R.; Zhang, W.; Liu, J.; Yu, Q.; Liu, W.; Huang, X. Isolation, Purification, Structural Characterization and Antitumor Activities of a Polysaccharide from *Lilium Davidii* Var. *Unicolor* Cotton. *J. Mol. Struct.* **2022**, *1261*, 132941. [[CrossRef](#)]
24. Szymanska-Chargot, M.; Zdunek, A. Use of Ft-Ir Spectra and Pca to the Bulk Characterization of Cell Wall Residues of Fruits and Vegetables Along a Fraction Process. *Food Biophys.* **2013**, *8*, 29–42. [[CrossRef](#)] [[PubMed](#)]
25. Chaturvedi, K.; Yadav, S.K. Ultrasonication Assisted Salt-Spices Impregnation in Black Carrots to Attain Anthocyanins Stability, Quality Retention and Antimicrobial Efficacy on Hot-Air Convective Drying. *Ultrason. Sonochem.* **2019**, *58*, 104661.
26. Liu, N.; Yang, W.; Li, X.; Zhao, P.; Liu, Y.; Guo, L.; Huang, L.; Gao, W. Comparison of Characterization and Antioxidant Activity of Different Citrus Peel Pectins. *Food Chem.* **2022**, *386*, 132683. [[CrossRef](#)]
27. Hastuti, B.; Totiana, F.; Winiasih, R. The Role of Pectin in Pb Binding by Carrot Peel Biosorbents: Isotherm Adsorption Study. In Proceedings of the 12th Joint Conference on Chemistry, Semarang, Indonesia, 19–20 September 2017. [[CrossRef](#)]
28. Koziol, A.; Sroda-Pomianek, K.; Gorniak, A.; Wikiera, A.; Cyprych, K.; Malik, M. Structural Determination of Pectins by Spectroscopy Methods. *Coatings* **2022**, *12*, 546. [[CrossRef](#)]
29. Wang, W.; Ma, X.; Jiang, P.; Hu, L.; Zhi, Z.; Chen, J.; Ding, T.; Ye, X.; Liu, D. Characterization of Pectin from Grapefruit Peel: A Comparison of Ultrasound-Assisted and Conventional Heating Extractions. *Food Hydrocoll.* **2016**, *61*, 730–739. [[CrossRef](#)]
30. Sucheta Misra, N.N.; Yadav, S.K. Extraction of Pectin from Black Carrot Pomace Using Intermittent Microwave, Ultrasound and Conventional Heating: Kinetics, Characterization and Process Economics. *Food Hydrocoll.* **2020**, *102*, 105592. [[CrossRef](#)]
31. Feng, Y.; Tan, C.P.; Zhou, C.; Yagoub, A.E.A.; Xu, B.; Sun, Y.; Ma, H.; Xu, X.; Yu, X. Effect of Freeze-Thaw Cycles Pretreatment on the Vacuum Freeze-Drying Process and Physicochemical Properties of the Dried Garlic Slices. *Food Chem.* **2020**, *324*, 126883. [[CrossRef](#)]
32. Xu, X.; Zhang, L.; Yagoub, A.A.E.; Yu, X.; Ma, H.; Zhou, C. Effects of Ultrasound, Freeze-Thaw Pretreatments and Drying Methods on Structure and Functional Properties of Pectin During the Processing of Okra. *Food Hydrocoll.* **2021**, *120*, 106965. [[CrossRef](#)]
33. Celus, M.; Kyomugasho, C.; Van Loey, A.M.; Grauwet, T.; Hendrickx, M.E. Influence of Pectin Structural Properties on Interactions with Divalent Cations and Its Associated Functionalities. *Compr. Rev. Food Sci. Food Saf.* **2018**, *17*, 1576–1594. [[CrossRef](#)] [[PubMed](#)]
34. Sajjaanantakul, T.; Van Buren, J.P.; Downing, D. Effect of Methyl Ester Content on Heat Degradation of Chelator-Soluble Carrot Pectin. *J. Food Sci.* **1989**, *54*, 1272–1277. [[CrossRef](#)]
35. Cui, J.; Zhao, C.; Feng, L.; Han, Y.; Du, H.; Xiao, H.; Zheng, J. Pectins from Fruits: Relationships between Extraction Methods, Structural Characteristics, and Functional Properties. *Trends Food Sci. Technol.* **2021**, *110*, 39–54. [[CrossRef](#)]
36. De Roeck, A.; Mols, J.; Duvetter, T.; Van Loey, A.; Hendrickx, M. Carrot Texture Degradation Kinetics and Pectin Changes During Thermal versus High-Pressure/High-Temperature Processing: A Comparative Study. *Food Chem.* **2010**, *120*, 1104–1112. [[CrossRef](#)]
37. Christiaens, S.; Van Buggenhout, S.; Vandevenne, E.; Jolie, R.; Van Loey, A.M.; Hendrickx, M.E. Towards a Better Understanding of the Pectin Structure-Function Relationship in Broccoli During Processing: Part II—Analyses with Anti-Pectin Antibodies. *Food Res. Int.* **2011**, *44*, 2896–2906. [[CrossRef](#)]
38. Feng, W.; Kita, D.; Peaucelle, A.; Cartwright, H.N.; Doan, V.; Duan, Q.; Liu, M.-C.; Maman, J.; Steinhorst, L.; Schmitz-Thom, I.; et al. The Feronia Receptor Kinase Maintains Cell-Wall Integrity during Salt Stress through Ca<sup>2+</sup> Signaling. *Curr. Biol.* **2018**, *28*, 666–675. [[CrossRef](#)] [[PubMed](#)]
39. Moens, L.G.; De Laet, E.; Van Wambeke, J.; Van Loey, A.M.; Hendrickx, M.E.G. Pulsed Electric Field and Mild Thermal Processing Affect the Cooking Behaviour of Carrot Tissues (*Daucus Carota*) and the Degree of Methylsterification of Carrot Pectin. *Innov. Food Sci. Emerg. Technol.* **2020**, *66*, 102483. [[CrossRef](#)]
40. Christiaens, S.; Van Buggenhout, S.; Houben, K.; Fraeye, I.; Van Loey, A.M.; Hendrickx, M.E. Towards a Better Understanding of the Pectin Structure-Function Relationship in Broccoli during Processing: Part I-Macroscopic and Molecular Analyses. *Food Res. Int.* **2011**, *44*, 1604–1612. [[CrossRef](#)]
41. Moens, L.G.; Huang, W.; Van Loey, A.M.; Hendrickx, M.E.G. Effect of Pulsed Electric Field and Mild Thermal Processing on Texture-Related Pectin Properties to Better Understand Carrot (*Daucus Carota*) Texture Changes during Subsequent Cooking. *Innov. Food Sci. Emerg. Technol.* **2021**, *70*, 102700. [[CrossRef](#)]

42. Xiao, M.; Yi, J.; Bi, J.; Lv, J.; Zhou, L.; Zhou, M. Influence of Different Dehydration Processes on the Texture and Pectin Characteristics of Apple Chips. *Mod. Food Sci. Technol.* **2017**, *33*, 157–162+117.
43. Sun, Y.; Kang, X.; Liang, D.; Chen, F.; Hu, X. Study on Effect and Mechanism of High Pressure Processing on Hardness of Fresh-Cut Carrot. *Sci. Technol. Food Ind.* **2017**, *38*, 200–204+208.
44. Yi, J.; Bi, J.; Liu, X.; Lv, J.; Zhou, M.; Wu, X.; Zhao, Y.; Du, Q. A Review: Domain Fine Structure of Pectic Polysaccharides. *Food Sci.* **2020**, *41*, 292–299.
45. Nagano, T.; Hirotsuka, M.; Mori, H.; Kohyama, K.; Nishinari, K. Dynamic Viscoelastic Study on the Gelation of 7 S Globulin from Soybeans. *J. Agric. Food Chem.* **1992**, *40*, 941–944. [[CrossRef](#)]
46. Yi, J.; Lv, J.; Bi, J.; Zhou, L.; Wu, X.; Zhou, M. Research Process of Structure and Function Relationship of Pectin in Processed Fruits and Vegetables. *J. Chin. Inst. Food Sci. Technol.* **2017**, *17*, 175–181.
47. Zhang, L.; Ye, X.; Ding, T.; Sun, X.; Xu, Y.; Liu, D. Ultrasound Effects on the Degradation Kinetics, Structure and Rheological Properties of Apple Pectin. *Ultrason. Sonochem.* **2013**, *20*, 222–231. [[CrossRef](#)]
48. Binnig, G.; Quate, C.F.; Gerber, C. Atomic Force Microscope. *Phys. Rev. Lett.* **1986**, *56*, 930. [[CrossRef](#)]
49. Cybulska, J.; Zdunek, A.; Kozio, A. The Self-Assembled Network and Physiological Degradation of Pectins in Carrot Cell Walls. *Food Hydrocoll.* **2015**, *43*, 41–50. [[CrossRef](#)]
50. Zhang, H.; Nie, S.; Guo, Q.; Wang, Q.; Cui, S.W.; Xie, M. Conformational Properties of a Bioactive Polysaccharide from *Ganoderma Atrum* by Light Scattering and Molecular Modeling. *Food Hydrocoll.* **2018**, *84*, 16–25. [[CrossRef](#)]

**Disclaimer/Publisher’s Note:** The statements, opinions and data contained in all publications are solely those of the individual author(s) and contributor(s) and not of MDPI and/or the editor(s). MDPI and/or the editor(s) disclaim responsibility for any injury to people or property resulting from any ideas, methods, instructions or products referred to in the content.